

Structure of TiAlN Reactive Sputtered Coatings

V.N. Denisov^{1,2,*}, B.N. Mavrin², E.A. Vinogradov², S.N. Polyakov¹, A.N. Kirichenko¹, K.V. Gogolinsky¹,
A.S. Useinov¹, V.D. Blank¹, V. Godinho^{3,4}, D. Philippon³, A. Fernandez³

¹ *Technological Institute for Superhard and Novel Carbon Materials, Troitsk, Moscow region, 142190 Russia*

² *Institute of Spectroscopy of RAS, Troitsk, Moscow region, Phizicheskaya street 5, 142190 Russia*

³ *Instituto de Ciencia de Materiales de Sevilla CSIC-US Avenida Americo Vespucio 49, 41092 Sevilla, Spain*

⁴ *Université Libre de Bruxelles Faculty of Applied Sciences, Chemicals and Materials Department, Avenue F.D.Roosevelt, 50 (CP165/63) 1050 Brussels, Belgium*

(Received 19 November 2011; published online 14 March 2012)

The Raman spectra, X-ray diffraction and hardness of the TiAlN films co-deposited on the steel substrates by reactive sputtering from Ti and Al targets in a mixture of N₂ + Ar gas with two magnetrons at room temperature have been studied. From Raman spectra it is found that the position of high-frequency bands in vibrational spectra was located at 700-730 cm⁻¹ or in the region of 830 – 850 cm⁻¹ depending on the deposition parameters whereas it is not exceed 630 cm⁻¹ from TiAlN of NaCl – structure. It is found the two-phase structure of coatings: a small quantity of NaCl-type structure of TiAlN (TiN) and the disordered structure of the chains of polyhedra [TiN_x] with $x = 5$ and $x = 4$. The chains of polyhedra [TiN_x] with $x = 4$ are mainly formed at large discharge power of Al(Ti) target or at small content of N₂ gas.

Keywords: Coating, Hardness, Reactive Sputtering, TiAlN, X-Ray Diffraction, Raman Spectroscopy.

PACS numbers: 62.20.F, 62.20 – x, 78.30Ly, 78.30. – j, 61.05.C,
61.05.cp

1. INTRODUCTION

Titanium-aluminium nitrides are technologically important for different application fields such as wear-resistant and optical coatings. The TiAlN coatings find a continuously interest due to its high hardness, wear resistance and low oxidation rates. TiN is a NaCl-structure and it has metallic conductivity at room temperature [1, 2]. AlN is crystallized in a wurtzite structure (w-AlN) and it may form the metastable rocksalt structure at high pressure [3]. The hardness of TiN is 21.6 GPa, while that of AlN is only 12.3 GPa [4]. Due to the structural refinement of TiAlN alloy the addition of Al atoms in TiN improves its hardness and the high-temperature oxidation resistance. However, for higher Al concentration the formation of w-AlN, which is softer than fcc-TiAlN, results in a significant reduction of the film hardness.

The structure of TiAlN coatings depends strongly on the deposition parameters, in particular, on the Ti/Al ratio, the discharge power, deposition gas, substrate temperature, etc. In this work a systematic study on the influence of deposition parameters on the structure of TiAlN coatings is presented.

Raman spectra and X-ray diffraction of TiAlN coatings were earlier studied by other authors for the TiN/AlN superlattices [5], TiAlN alloys [6-9], TiAlN/CrN multilayers [7] and TiAlN-Si₃N₄ nanocomposite [10]. In these works, [5-10] results are given for coatings prepared at fixed Ti/Al ratio, with substrate temperature above room temperature and at invariable content of N₂ gas.

2. EXPERIMENTAL DETAILS

The TiAlN films were co-deposited on sputter cleaned steel substrates by reactive sputtering from pure Ti and pure Al targets (Kurt Lesker 99.99 %) in a mixture of N₂+Ar gas. Deposition was performed in a vacuum chamber equipped with two magnetrons driven by dc power. Table 1 summarizes the deposition conditions.

Table 1 – Deposition conditions

| No | | |
|----|---------------------------|---|
| 1 | Base pressure | 10–4 Pa |
| 2 | Target substrate distance | 10 cm |
| 3 | Substrate cleaning | 400V at 7Pa Ar for 15 min |
| 4 | Target cleaning | 600W at 7Pa Ar for 15 min |
| 5 | Power supply (Ti, Al) | 200–600 W d.c |
| 6 | Sputtering gas | %N ₂ /(N ₂ +Ar) = 15, 30, 70% |
| 7 | Deposition time | 5-150 min |

The power supplied to the two targets varied from 200 to 600 W and different gas mixtures were used in order to obtain coatings with different composition. The composition of the coatings was evaluated by XPS (not presented here), the Ti_{1-x}Al_xN present compositions ranging from $x = 0.07$ to 0.60. The effect of deposition time on the structure of the TiAlN films was also investigated. For thick coatings, a TiAl adhesion layer was deposited prior to the coating.

The microstructure of the coatings was investigated by XRD. The XRD measurements were performed in the Rigaku D / max-RC equipped with a 12 kW X-ray source with a rotary anode using monochromatic Cu K α radiation and the graphite crystal-analyser. The grazing incidence asymmetrical Bragg diffraction (GIABD) with the parallel beam optics was employed for phase composition and chemical homogeneity investigations. Incidence angles of 1 and 0.5 were used.

The Raman spectra were excited with the line at 514.5 nm of an Ar-laser. The spectrograph TRIAX 552 with special corrective optics, the Notch filters and CCD camera were used for the investigation of the Raman scattering light. The spectral resolution was about 3 cm⁻¹. We have used the setup of micro-Raman spectroscopy with a microscope which provided a focus diameter in the micrometer range and a large scatter-

* denisovvn@ntcstm.troitsk.ru

ing collection angle. The mechanical properties and surface topography were investigated using the scanning nano-hardness tester NanoScan – 3D. The hardness and elastic modulus values were measured with the instrumented nanoindentation test according to ISO 14577.

3. RESULTS AND DISCUSSION

3.1 X-Ray Diffractometry

Figure 1 presents the X-ray diffraction pattern for samples deposited under different power rate and deposition times resulting in different thickness. Peak positions for reference compounds of c-TiN and c-TiAlN are marked.

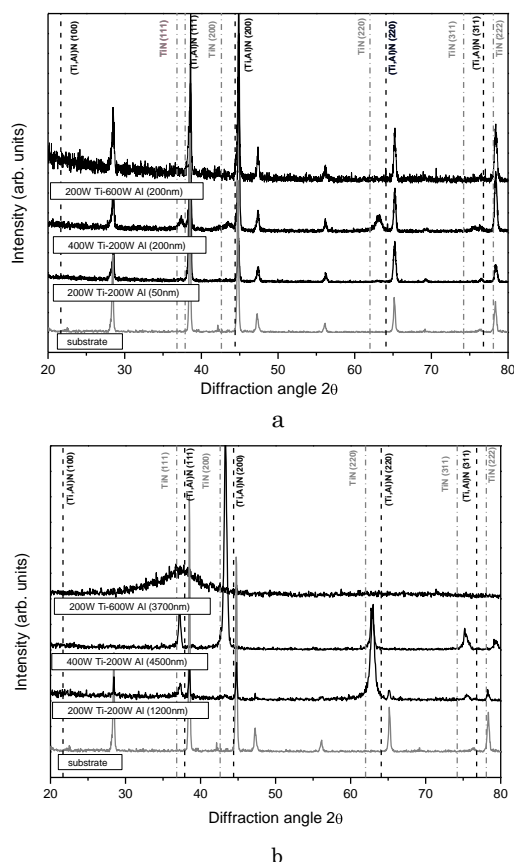


Fig. 1 – X-ray diffraction patterns for samples prepared at different power rate and deposition times: thinner coatings, incidence angle of 0.5°(a); thicker coatings, incidence angle of 1°(b)

A part from substrate peaks, NaCl-type of (TiAl)N (non stoichiometric) diffraction peaks can be identified as well. In both cases thinner and thicker coatings, the increase in Ti power results in an increase of crystallinity of the coating, and the preferential orientation changes from (111) to (200). When the power in the Al target is increased to 600 W the coating becomes more amorphous.

3.2 Raman Spectroscopy

Raman spectra of obtained TiAlN coatings are presented at Figures 2-7. A narrow band at 520 cm^{-1} was seen in the Raman spectra from TiAlN thin coatings (≤ 100 nm) (Fig. 2). It disappeared gradually as the coating thickness increased. We assign it to the Raman

scattering from the substrate. Apart from this narrow band only the broad bands were observed in the Raman spectra from TiAlN coatings (Fig. 2-7). Depending on the deposition process the position of high-frequency band in the Raman spectra was about 700 cm^{-1} or in the region of 830-850 cm^{-1} . When the bands at 830-850 cm^{-1} were present in the spectrum, the broad bands in the region of 600-630 cm^{-1} also appeared and these two regions of the broad bands have formed the poorly structured background due to the overlapping (Fig. 2-7).

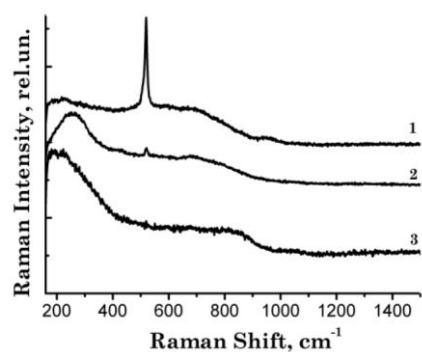


Fig. 2 – Raman spectra of TiAlN coatings at Ti discharge power of 200 W and 15%N₂. Where 1 – 200 W Al, 2 – 400 W Al, 3 – 600 W Al

It is known [1] that the Raman bands of TiN are due to a contribution of the phonon density of states from the acoustic modes (225 (TA) and 310 (LA) cm^{-1}) and the optic modes (540 cm^{-1}). When Al atoms are added to TiN lattice the structure of NaCl-type is maintained and Ti atoms are substituted by Al atoms [11]. As in the case of TiN-NbN [8], TiAlN-CrN [7] and CrAlN [12], we believe that the Raman bands in the spectra from TiAlN alloys are assigned to vibrations of Ti-N bonds, and the influence of Al doping is displayed in a high-frequency shift of optic modes of TiN. The stress in coatings may also lead to the high-frequency shift of bands in spectra. Therefore we assign the Raman bands in the region of 600 – 630 cm^{-1} to the optic vibrations of Ti-N bond in TiAlN coatings with a NaCl-structure.

An appearance of broad bands in the regions of 700-730 and 830-850 cm^{-1} can not be explained by a substitution of Ti atoms by Al atoms in the structure of NaCl-type. Supposing the assignment of these bands to vibrations of Ti-N bonds, the significant rise of their frequencies may be due to the break of NaCl-type of TiN structure and the formation of the disordered structure with the chains of polyhedra [TiN_x] with the less number of N atoms around Ti than 6. It is known that the vibrational frequency is increased with a decrease of the coordination number. Therefore one can assume that the bands at 700-730 cm^{-1} correspond to chains with $x = 5$ and at 830-850 cm^{-1} to chains with $x = 4$.

At first we shall consider the Raman spectra from TiAlN coatings produced at the constant ration Ti/Al and at the increase of discharge power (Fig. 2). If the position of the high-frequency band is near 700 cm^{-1} and the intensity of acoustic and optic bands are comparable at 200 W discharge power, then two bands at 610 and 840 cm^{-1} and the essential rise of the intensity

of acoustic modes may be seen in the Raman spectra from coatings produced at 400 and 600 W power. Note the band at 700 cm^{-1} is overlapped with the broad band at 610 cm^{-1} . One can assume two-phase composition of coatings produced at all powers: TiAlN of NaCl-structure (the band at 610 cm^{-1}) and a phase with chains of $[\text{TiN}_x]$ polyhedra with $x=5$ (the band at 700 cm^{-1}) and $x=4$ (the band at 840 cm^{-1}). In Fig. 2, as in Fig. 3 and 4, the Raman spectra are shown for coatings of approximately similar thickness.

In the Raman spectra from TiAlN coatings prepared at fixed Ti power (200 W) and at various Al powers (Fig. 3) one can see also two-phase structure and the quantity of the NaCl-structure of TiAlN is decreased with the increase of Al power.

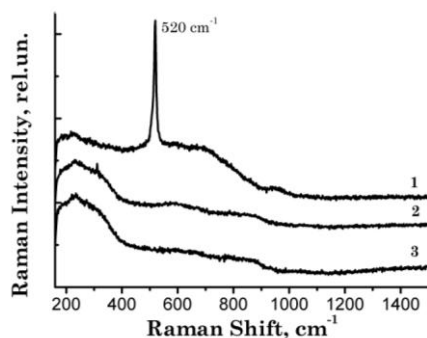


Fig. 3 – Raman spectra of $\text{Ti}_{0.5}\text{Al}_{0.5}\text{N}$ coatings at various Al and Ti discharge power and 15% N_2 . Where 1 – 200 W Al, 200 W Ti, 2 – 400 W Al, 400 W Ti, 3 – 600 W Al, 600 W Ti

Besides the type of chains changes from $x=5$ to $x=4$, two-phase structure of TiAlN coatings produced at fixed Al power is also formed with the increase of Ti power (Fig. 4).

Fig. 5 shows the transformation of the Raman spectra from TiAlN coatings prepared at various content of N_2 gas. The position of the high-frequency band is equal to 700 cm^{-1} at 70% N_2 and 730 cm^{-1} at 30% N_2 . But two bands at 590 and 840 cm^{-1} and the noticeable increase of the intensity of acoustic modes are seen at 15% N_2 . We assume that the two-phase structure of TiAlN coating is formed at 15% N_2 .

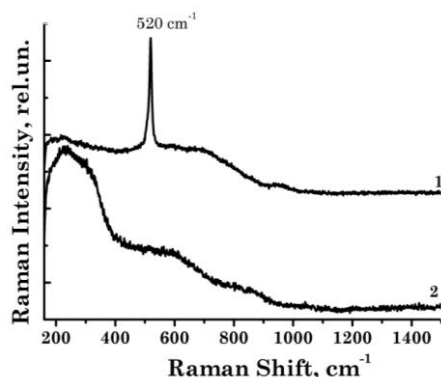


Fig. 4 – Raman spectra of TiAlN coatings at Al discharge power of 200 W and 15% N_2 and various Ti discharge power. Where 1 – 200 W Ti and thickness 125 nm, 2 – 400 W Ti and thickness 205 nm

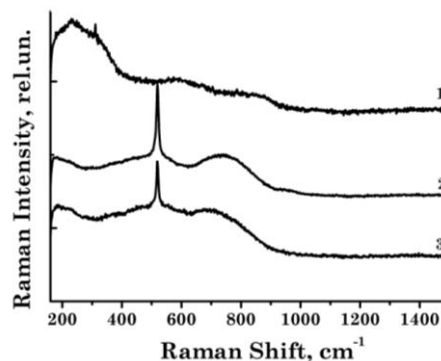


Fig. 5 – Raman spectra of TiAlN coatings at equal Ti/Al ratio and various N_2 content. Ti and Al discharge power is 400 W. 1 – 15% N_2 , 2 – 30% N_2 , 3 – 70% N_2 .

Most likely, two-phase structure with predominant content of chains $[\text{TiN}_5]$ is formed in TiAlN coatings prepared at 200 W Ti – 200 W Al power for thicknesses from 52 to 1200 nm (Fig. 6). One can see in the Raman spectra that the signal / noise ratio is higher in the coating of 52 nm thickness than for thicker coatings. Besides, the band at 730 cm^{-1} in the thin coating is more distinct than in the spectra from the thick coatings.

One can assume that the TiAlN alloys that is contiguous to the substrate is not only more homogeneous, but also it gives the resonance enhancement of the Raman intensity due to a change of electronic structure of TiN at Al doping or the electromagnetic enhancement on the metal-film boundary. It should be noted that the Fermi level in TiAlN alloys of NaCl – structure moves progressively down from the conduction band to the band gap as the alloy composition is varied from metallic TiN to wide-gap semiconductor AlN.

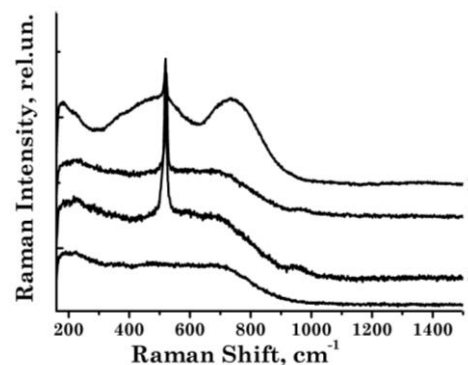


Fig. 6 – Raman spectra of TiAlN coatings at ratio Ti / Al = 1 and various thickness of coating. Ti and Al discharge power is 200 W, 15% N_2 . Thickness is: 1 – 52 nm, 2 – 100 nm, 3 – 125 nm, 4 – 1200 nm

The increase of the coating thickness doesn't lead also to the essential transformation of its structure at the ratio Al / Ti \neq 1 that one can see from the spectra for coatings with the ratio Al / Ti = 3 (Fig. 7). However, the spectrum from the thick coating (3700 nm) was weaker and the high-frequency optic modes in the region of $\sim 800\text{ cm}^{-1}$ are weak in comparison with the band at $\sim 600\text{ cm}^{-1}$.

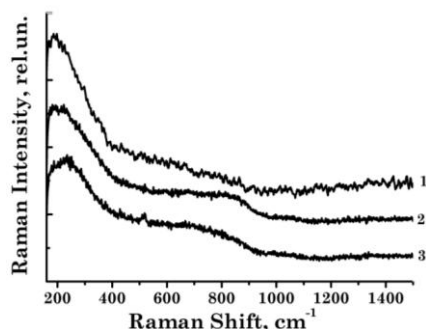


Fig. 7 – Raman spectra of TiAlN coatings at ratio Ti / Al = 1 / 3 (200 W on Ti, 600 W on Al target, 15 % N₂) and various thickness of coatings. 1 – 3700 nm, 2 – 180 nm, 3 – 90 nm

3.3 Nano-Hardness Tests

Young module E , hardness H and elastic modulus R under loading P and thickness of coatings h are given in Table 2.

Table 2 – NanoScan3D test results.

| Coating preparation condition | P , mN | h , nm | E , GPa | H , GPa | R , % |
|--|----------|----------|-----------|-----------|---------|
| 200 W Ti – 200 W Al, 15 % N ₂ | 1 | 80 | 118 | 5.1 | 40 |
| 400 W Ti – 400 W Al, 70 % N ₂ | 2 | 90 | 172 | 8.9 | 52 |
| 200 W Ti – 400 W Al, 30 % N ₂ | 2 | 130 | 114 | 4.4 | 36 |
| 400 W Ti – 200 W Al, 15 % N ₂ | 5 | 190 | 146 | 5.4 | 35 |
| 200 W Ti – 600 W Al, 15 % N ₂ | 5 | 140 | 150 | 12.1 | 45 |

REFERENCES

1. W.°Sprengler, R.°Kaiser, A.N.°Christiansen, G.°Müller-Fogt, S.°Veprek, *Phys. Rev. B.* **17**, 1095 (1978).
2. B.O.°Johanson, J.-E.°Sundgren, J.E.°Greene, A.°Rockett, S.A.°Barnett, *J. Vac. Sci. Technol.* **A3**, 303 (1985).
3. Q.°Xia, H.°Xia, A.L.°Ruoff, *J. Appl. Phys.* **73**, 8198 (1993).
4. *CRC Materials Science and Engineering Handbook*, (Ed. J.F.°Shackelford, W.°Alexander, J.S.°Park) (Boca Raton: CRC Press: 1994).
5. M.°Bernard, A.°Deneuve, O.°Thomas, P.°Gergaud, P.°Sandstrom, J. Birch, *Thin Solid Films* **380**, 252 (2000).
6. C.P.°Constable, J.°Yarwood, W.-D.°Münz, *Surf. Coat. Tech.* **116**, 155 (1999).
7. H.C.°Barshilia, K.S.°Rajam, *J. Mater. Res.* **19**, 3196 (2004).
8. H.C.°Barshilia, K.S.°Rajam, *J. Appl. Phys.* **98**, 014311 (2005).
9. B.°Subramanian, K.°Ashok, P.°Kuppusami, C.°Sanjeeviraja, M.°Jayachandran, *Cryst. Res. Technol.* **43**, 1078 (2008).
10. H.C.°Barshilia, B.°Deepthi, K.S.°Rajam, *Vacuum* **81**, 479 (2006).
11. V.°Podgursky, B.°Torp, R.°Traksmaa, R.°Veinthal, M.°Viljus, O.°Coddet, M.°Morstein, A.°Gregor, P.°Kulu, *Material Science (Medžiagotyra)*, **11**, 352 (2005).
12. H.C.°Barshilia, N.°Selvakumar, B.°Deepthi, K.S.°Rajam, *Surf. Coat. Tech.* **201**, 2193 (2006).
13. L.°García-González, M. G.°Garnica-Romo, J.°Hernández-Torres, F.°J.°Espinoza-Beltrán, *Braz. J. Chem. Eng.* **24**, 249 (2007).

Our results are in agreement with the hardness obtained for TiAlN coatings deposited on substrates at 22 °C [13].

4. CONCLUSIONS

The investigations of Raman spectra and X-ray diffraction of TiAlN coatings on the steel substrates deposited at room temperature allow us to find the structural transformation of coatings in dependence on the deposition process. XRD has shown multiphase composition of coatings. The different structures of coatings were displayed in the position of high-frequency Raman bands in the region $> 500 \text{ cm}^{-1}$. It is assumed that the Raman band at $600\text{-}630 \text{ cm}^{-1}$ corresponds to a NaCl – structure of TiAlN alloy and the appearance of Raman broad bands above 630 cm^{-1} could be due to a formation of chains of polyhedra [TiN_x] with $x = 4$ or 5. It was shown two-phase structure of coatings: a small quantity of NaCl – structure and the disordered structure of chains [TiN_x] with $x = 4$ or 5. The chains of polyhedra [TiN_x] with $x = 4$ are mainly formed at large discharge power of Al(Ti) target or at small content of N₂ gas.

ACKNOWLEDGEMENTS

Authors thank the financial support from EC (project NOE EXCELL), Spanish Ministry MICINN (CONSOLIDER FUNCOAT) and Junta de Andalucía.